Matthews, B. W. (1972) *Macromolecules 5*, 818.
McManus, O. B., Musick, J. R., & Gonzalez, C. (1981) *Neurosci. Lett. 24*, 57.
Nerdal, W., Hare, D. R., & Reid, B. R. (1988) *J. Mol. Biol. 201*, 717.
Olivera, B. M., Gray, W. R., Zeikus, R., McIntosh, J. M., Varga, J., Rivier, J., de Santos, V., & Cruz, L. J. (1985) *Science 230*, 1338.
Pardi, A., Hare, D. R., Selsted, M. E., Morrison, R. D., Bassolino, D. A., & Bach, A. C., II (1988) *J. Mol. Biol. 201*, 625.
Piantini, U., Sorensen, O. W., & Ernst, R. R. (1982) *J. Am. Chem. Soc. 104*, 6800.
Rich, D. H., Kawai, M., & Jasensky, R. D. (1983) *Int. J. Pept. Protein Res. 21*, 35.
Richardson, J. (1981) *Adv. Protein Chem. 34*, 167.
Shaka, A. J., & Freeman, R. (1983) *J. Magn. Reson. 51*, 169.
Stenlake, J. B. (1981) in *Burger's Medicinal Chemistry* (Wolff, M. B., Ed.) p 431, Wiley, New York.
Van Gunsteren, W. F., & Berendson, H. J. C. (1977) *Mol. Phys. 34*, 1311.
Weiner, P., & Kollman, P. A. (1981) *J. Comput. Chem. 2*, 287.
Weiner, S. J., Kollman, P. A., Case, D. A., Singh, U. C., Ghio, M. C., Alagona, G., Profeta, S., & Weiner, P. (1984) *J. Am. Chem. Soc. 106*, 765.
Wüthrich, K. (1986) *NMR of Proteins and Nucleic Acids*, Wiley, New York.
Wüthrich, K., Billeter, M., & Braun, W. (1983) *J. Mol. Biol. 169*, 949.
Wüthrich, K., Billeter, M., & Braun, W. (1984) *J. Mol. Biol. 180*, 715.
Yang, C. C., Chang, C. C., & Liou, I. F. (1974) *Biochim. Biophys. Acta 365*, 1.

Characterization of Lens α-Crystallin Tryptophan Microenvironments by Room Temperature Phosphorescence Spectroscopy†

Jeffrey W. Berger and Jane M. Vanderkooi*

Department of Biochemistry and Biophysics, School of Medicine, University of Pennsylvania, Philadelphia, Pennsylvania 19104

Received September 23, 1988; Revised Manuscript Received March 14, 1989

ABSTRACT: Room temperature phosphorescence techniques were used to study the structural and dynamic features of the tryptophan residues in bovine α-crystallin. Upon excitation at 290 nm, the characteristic signature of tryptophan phosphorescence was observed with an emission maximum at 442 ± 2 nm. The phosphorescence intensity decay was biphasic with lifetimes of 5.4 ms (71%) and 42 ms (29%). Phosphorescence quenching measurements strongly suggest that each component corresponds to one class of tryptophans with the more buried residues having the longer emission lifetime. Three small-molecule quenchers were surveyed, and in order of increasing quenching efficiency: iodide < nitrite < acrylamide. A heavy-atom effect was observed in iodide solutions, and an upper limit of 5% was placed on the quantum yield of triplet formation in iodide-free solutions, while the phosphorescence quantum yield was estimated to be $\sim 3.2 \times 10^{-4}$. The temperature dependence of the phosphorescence lifetime was measured between 5 and 40 °C. Arrhenius plots exhibited discontinuities at 26 and 29 °C for the short- and long-lived components, respectively, corresponding to abrupt transitions in segmental flexibility. Denaturation studies revealed conformational transitions between 1 and 2 M guanidine hydrochloride, and 4 and 6 M urea. Long-lived phosphorescence lifetimes of 3 and 7 ms were measured in 6 M guanidine hydrochloride and 8 M urea, respectively, suggesting that some structural features are preserved even at very high concentrations of denaturant. Our studies demonstrate the sensitivity of room temperature phosphorescence spectroscopy to the structure of α-crystallin, and the applicability of this technique for monitoring conformational changes in lens crystallin proteins.

Eye lens fibers contain a highly concentrated solution of lens-specific crystallin proteins, and the short-range ordering of the crystallins is essential for the maintenance of lens transparency and for proper focusing of light on the retina (Tardieu & Delaye, 1988). Cataracts are characterized by aggregation and insolubilization of crystallin proteins, and it is believed that protein conformational changes precede the onset of opacification. A variety of biochemical and spectroscopic techniques have been used to probe the structure of lens crystallins, and to monitor the conformational changes associated with aging (Lerman & Borkman, 1978; Ozaki et al., 1983; Libondi et al., 1986; Liang, 1987) and cataract (Harding, 1972, 1981; McNamara & Augusteyn, 1984).

α-Crystallin is an aggregate composed of A and B subunits each with a molecular weight of ~20000 (Bloemendal, 1981). α-A_2 and α-B_2 are the primary gene products, while α-A_1 and α-B_1 arise via posttranslational adenosine cyclic 3′,5′-phosphate (cAMP)[1]-dependent phosphorylation (Chiesa et al., 1988).

† This work was supported by an NIH Cell and Molecular Biology training grant (J.W.B.) and by NIH Grant GM 21487 (J.M.V.).
* To whom correspondence should be addressed.

[1] Abbreviations: cAMP, adenosine cyclic 3′,5′-phosphate; SDS-PAGE, sodium dodecyl sulfate–polyacrylamide gel electrophoresis; Gdn-HCl, guanidine hydrochloride.

0006-2960/89/0428-5501$01.50/0

Sequence analysis has shown that A_2 subunits contain one tryptophan at position 9 and that B_2 subunits contain two tryptophans at positions 9 and 60 (van der Ouderaa et al., 1973, 1974). Models for the quaternary structure of α-crystallin have been proposed (Siezen et al., 1980; Tardieu et al., 1986); however, a complete description of the structure and conformation has yet to be presented.

Pioneering studies by Saviotti and Galley (1974) and further work by Vanderkooi et al. (1987) have established that protein tryptophan phosphorescence can be measured at moderate temperatures in deoxygenated solutions. Recent studies on model systems have demonstrated that room temperature phosphorescence is exquisitely sensitive to tryptophan microenvironment and protein conformation (Kishner et al., 1983; Strambini & Gonnelli, 1986; Strambini et al., 1987). Since the differential susceptibility of the crystallins to cataractogenic agents such as ultraviolet light (Andley & Chapman, 1986; Mandal et al., 1988) and sugar (Liang & Chakrabarti, 1981; Liang et al., 1986) has been attributed to microenvironmental heterogeneity, it is of interest to probe the microenvironment of lens crystallin tryptophans with phosphorescence measurements at room temperature.

We present room temperature phosphorescence measurements of bovine α-crystallin in order to characterize more fully the microenvironments of the native tryptophan residues. In addition, the temperature dependence and the effects of chemical denaturants on the phosphorescence lifetime were studied to assess both structural stability and the applicability of room temperature phosphorescence spectroscopy for monitoring conformational changes of lens crystallin proteins.

Materials and Methods

Sample Preparation. α-Crystallin was obtained from Sigma Chemical Co. (St. Louis, MO) and was checked for purity by using SDS–PAGE (12% acrylamide) as per Laemmli (1970). Two characteristic bands at ~20 kDa were observed corresponding to the A and B subunits, and a third very weak band at ~17 kDa was identified which is thought to be a degradation product and is frequently observed in SDS gels of α-crystallin (van Kleef et al., 1976). The protein was estimated to be >95% pure and required no further purification. Room temperature phosphorescence spectra and lifetimes were measured on deoxygenated samples. Buffer solutions (0.1 M NaCl/0.01 M PO_4, pH 7) were first vacuum degassed and subsequently bubbled vigorously with oxygen-free argon. Protein solutions (0.5 mg/mL) were prepared, and an oxygen-consuming enzyme system of glucose oxidase (80 nM), catalase (16 nM), and 0.3% glucose was added to maintain deoxygenation and consume residual H_2O_2 (Englander et al., 1987). Finally, deoxygenated mineral oil was layered over the top of the sample to minimize the inward diffusion of oxygen.

Preparation of Denatured Samples. Denatured protein samples were prepared by dissolving α-crystallin in deoxygenated guanidine hydrochloride (Gdn-HCl, Sigma, grade 1) and urea solutions. Buffer solutions were vacuum degassed and bubbled vigorously prior to the addition of denaturant. The deoxygenating enzyme system was added both immediately preceding and following denaturant addition in order to eliminate the effect of reduced enzyme activity at higher denaturant concentrations. Subsequent preparation steps were conducted with argon flowing over the sample to exclude oxygen contamination. The pH was readjusted to 7.5, and the samples were allowed to incubate in the denaturant solution for 2 h at 25 °C.

Spectroscopic Measurements. Fluorescence spectra were acquired on a Perkin-Elmer 650-10S fluorescence spectrophotometer. Samples were excited at 295 nm, and the emission was scanned at 60 nm/min with an excitation and emission band-pass of 2 nm.

Room temperature phosphorescence spectra were measured on a Perkin-Elmer LS-5 spectrophotometer equipped with a PE 7500 professional computer. The excitation and emission slits were at 15 and 5 nm, respectively, and the first 0.5 ms of the emission was gated out in order to limit the contribution of the prompt fluorescence emission. Phosphorescence intensity decay curves were acquired on a home-built phosphorimeter which is fully described elsewhere (Green et al., 1988) with excitation at 290 nm. Normally, 200–300 repetitions were averaged in order to achieve an adequate signal, and the decay curves were fit to a sum of exponentials with ASYSTANT (Macmillan Software, NY) using a Gauss–Newton, least-squares curve-fitting algorithm. The goodness of the fit was judged by the sum of the squares of the residuals and the magnitude of the weighted χ^2 (Lakowicz, 1983).

Phosphorescence spectra at 77 K were recorded on the PE LS-5 from buffer solutions (0.1 M NaCl/0.01 M PO_4, pH 7) diluted (1:1 v/v) with glycerol to a final concentration of 1 mg/mL. The excitation and emission slits were reduced to 3 nm for greater resolution.

Temperature Dependence. The temperature dependence of the phosphorescence lifetime was measured between 5 and 40 °C. Beginning at 5 °C, the temperature of the sample was raised and allowed to equilibrate at the new temperature for 15 min.

Following the method of Kai and Imakubo (1979), the rate constant for excited-state deactivation is expressed as a sum of temperature-dependent and temperature-independent terms:

$$\tau_p^{-1} = k_p = k_0 + k_T \quad (1)$$

where τ_p is the phosphorescence lifetime, k_p is the rate constant for depopulation of the triplet state, and k_T and k_0 are the temperature-dependent and temperature-independent contributions to the overall decay rate. At moderate temperatures, $k_T \gg k_0$; hence, the temperature-dependent data was fit to an Arrhenius equation of the form

$$k_p \approx k_T = A \exp(-E_a/kT) \quad (2)$$

where A is in units of frequency (s^{-1}), E_a is the activation barrier in kilocalories per mole, k is the Boltzmann constant, and T is the absolute temperature. A and E_a were derived from best linear fits to Arrhenius plots of log k_p vs $1/T$.

Phosphorescence Quenching. Phosphorescence quenching measurements were performed by adding aliquots of 1 M acrylamide, 1 M nitrite, and 4 M iodide solutions. The iodide was maintained in its reduced form by the addition of 0.1 mM sodium thiosulfate to the concentrated iodide solution. The quencher solutions were deoxygenated according to procedures described above. Quenching constants were determined by measuring the reduction in phosphorescence lifetime with increasing quencher concentration. Intensity decay curves were fit to a sum of two exponentials, and quenching constants were determined from best linear regression fits to the Stern–Volmer equation modified for lifetime measurements (Lakowicz, 1983):

$$\tau_0/\tau = 1 + k_q\tau_0[Q] \quad (3)$$

where τ_0 is the phosphorescence lifetime in the absence of added quencher, τ is the measured lifetime, k_q is the bimolecular quenching constant, and [Q] is the quencher concentration. Quenching constants for the long- and short-lived components were derived independently by simultaneously

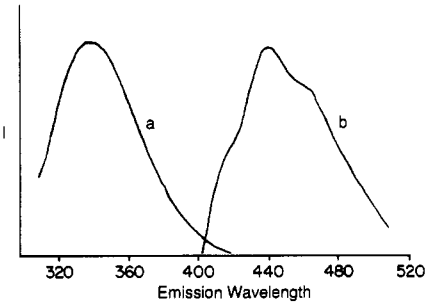

FIGURE 1: Fluorescence (a) and phosphorescence (b) emission spectra of bovine α-crystallin in 0.1 M NaCl/0.01 M PO_4 buffer, pH 7, at 20 °C. Excitation at 290 nm. For clarity, the spectra are normalized to unit intensity at their respective emission maxima.

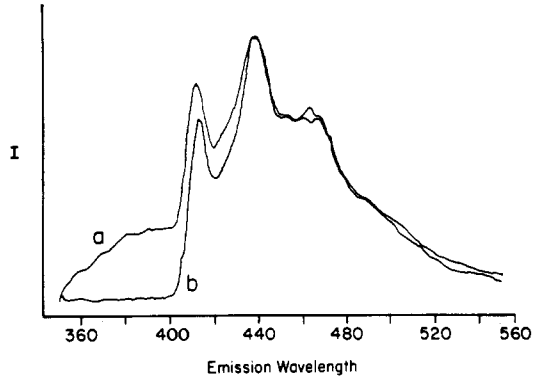

FIGURE 2: Phosphorescence spectra of α-crystallin in buffer (0.1 M NaCl/0.01 M PO_4, pH 7) diluted 1:1 v/v in glycerol at 77 K. Excitation at (a) 270 nm and (b) 295 nm. The spectra are normalized to unit intensity at the emission maxima.

measuring both components of the biphasic intensity decay.

The ability of iodide solvent to promote intersystem crossing via an external heavy-atom effect (Turro, 1978) was investigated by simultaneously measuring the fluorescence and phosphorescence intensities as a function of [I^-]. The fluorescence intensity was defined as the amplitude of the fluorescence at the emission maximum normalized to the amplitude of the fluorescence for iodide-free solvent. The phosphorescence intensity was calculated in two ways. First, the amplitude of the phosphorescence intensity decay curve at $t = 0$ was measured to observe the iodide perturbation of triplet formation. Second, the total phosphorescence intensity calculated as the area under the intensity decay curve was computed in order to monitor the effect of iodide on phosphorescence quantum yield.

Results

Fluorescence and Phosphorescence Spectra. The fluorescence and phosphorescence emission spectra of bovine α-crystallin at 20 °C are presented in Figure 1. The excitation spectra for fluorescence and phosphorescence (not shown) are virtually identical since both reflect $S_1 \leftarrow S_0$ transitions. The maximum of the fluorescence emission is at 337 ± 2 nm, which is consistent with the value of 335–336 nm reported by Liang and Chakrabarti (1982). The maximum of the phosphorescence emission occurs at 442 ± 2 nm with shoulders at 415–420 and 460–465 nm. The phosphorescence spectrum reflects the characteristic signature of room temperature tryptophan phosphorescence.

Low-temperature phosphorescence spectra are presented in Figure 2. At 295-nm excitation, the 0–0 band is observed at 412 ± 2 nm along with an emission maximum at 438 nm and a shoulder at ~465 nm. At 270-nm excitation, the features of the Trp phosphorescence are unchanged while tyrosine phosphorescence contributes to the emission in the 350–400-nm region. We attempted to resolve the 0–0 band into two or more components reflecting distinct Trp classes; however, even at an excitation and emission band-pass of 1 nm, distinct contributions could not be distinguished.

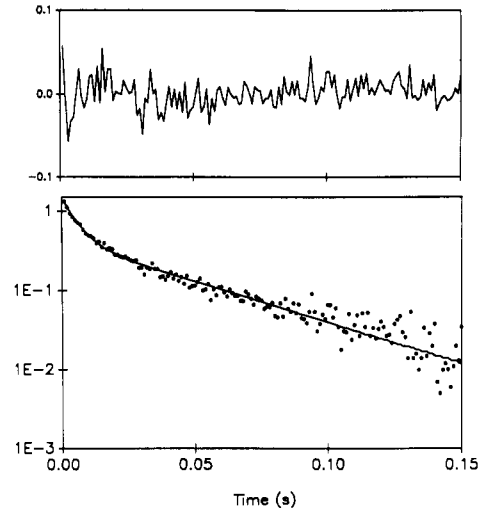

FIGURE 3: Phosphorescence intensity decay curves for α-crystallin. Conditions as described in Figure 1. The solid line is the best double-exponential fit ($\chi^2 = 0.67$) to the raw data, and the residuals are depicted above. A single exponential poorly fit the data ($\chi^2 = 52.8$).

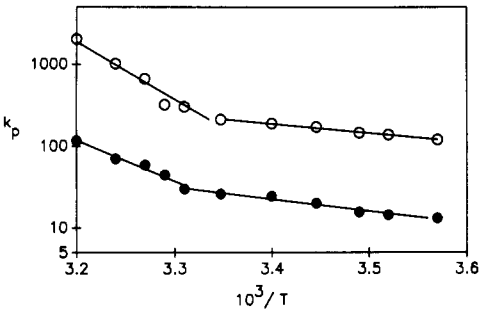

FIGURE 4: Arrhenius plot for the temperature dependence of the short-lived (○) and long-lived (●) components of the α-crystallin phosphorescence emission. Solid lines are best linear fits to the data above and below the transition temperatures.

Phosphorescence Lifetimes. The intensity decay curve for the phosphorescence emission of bovine α-crystallin at 20 °C is presented in Figure 3. The decay curve is clearly non-single-exponential, and a best double-exponential fit yielded lifetimes of 5.4 and 42 ms (±5%) with amplitude coefficients (arbitrary units) of 1.04 (71%) and 0.42 (29%), respectively. Fitting to a sum of three exponentials did not significantly improve the fit as judged by the sum of the squares of the residuals.

Arrhenius plots for the temperature dependence of the short- and long-lived components of the phosphorescence emission are depicted in Figure 4. An abrupt transition is observed at ~26 °C for the short-lived component and at ~29 °C for the long-lived component. Fits to the low-temperature data yielded $E_a = 5.1$ kcal/mol and $A = 1.2 \times 10^6$ s^{-1} for the short-lived component and $E_a = 6.7$ kcal/mol and $A = 2.1 \times 10^6$ s^{-1} for the long-lived phosphorescence component. Above the transition temperature, $E_a = 32$ kcal/mol and $A = 5 \times 10^{25}$ s^{-1} for the short-lived component and $E_a = 23$ kcal/mol and $A = 1.8 \times 10^{18}$ s^{-1} for the long-lived component.

Phosphorescence Quenching by Added Small Molecules. Added small-molecule quenching of the native tryptophan phosphorescence allowed for evaluation of tryptophan acces-

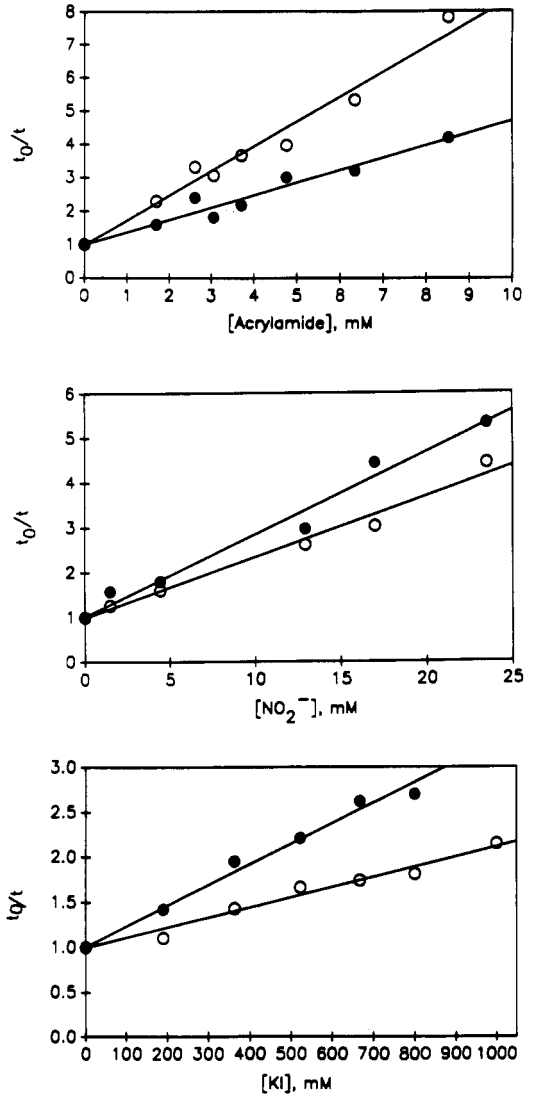

FIGURE 5: Stern–Volmer plots for acrylamide, nitrite, and iodide quenching of the short-lived (○) and long-lived (●) components of the α-crystallin phosphorescence emission. Conditions as described in Figure 1.

Table I: Lifetime and Quenching Data for the Phosphorescence of Bovine α-Crystallin at 20 °C[a]

	lifetime		quenching constant		
component	f	τ	acrylamide	nitrite	iodide
short-lived	0.71	5.4	1.5×10^5	2.3×10^4	2.6×10^2
long-lived	0.29	42	9.3×10^3	3.5×10^3	6.3×10

[a] f is the amplitude of the exponential component with lifetime (τ, ms). Quenching constants are in units of M^{-1} s^{-1}.

sibility. Stern–Volmer plots for phosphorescence quenching by acrylamide, nitrite, and iodide are presented in Figure 5, and the bimolecular quenching constants for the long- and short-lived phosphorescence components were computed (Table I). The tryptophans were most accessible to the neutral acrylamide molecule, and most protected from the hydrated iodide ion. As a control, the phosphorescence emission in 500 mM NaCl buffer was measured to investigate ionic effects, and no change in the phosphorescence intensity or lifetimes was observed.

While the phosphorescent tryptophans are highly protected from iodide quenching, a clear heavy-atom effect is observed (Figure 6A). Over the domain $0 < [I^-] < 800$ mM, the fluorescence intensity decreases by ~30% while the initial phosphorescence intensity increases 5-fold. The total phosphorescence intensity increases by 230%.

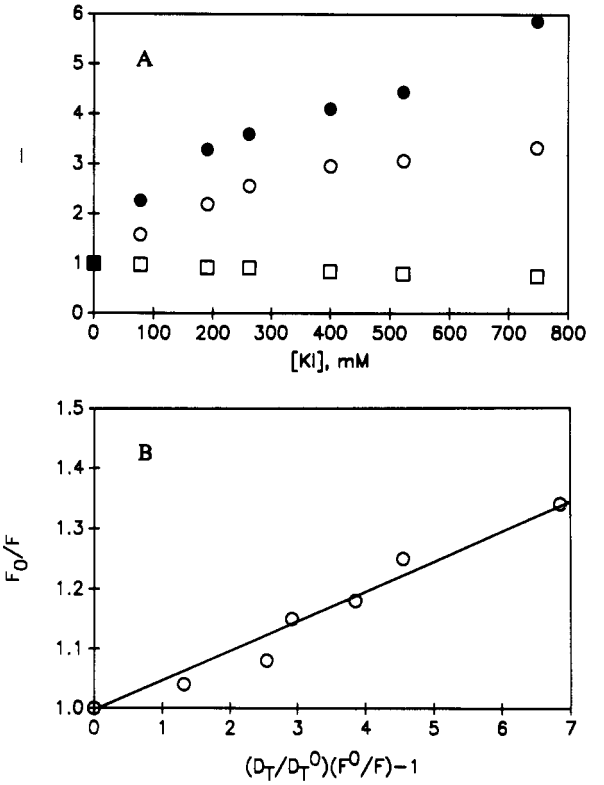

FIGURE 6: Demonstration of the heavy-atom effect for α-crystallin in iodide solvent. (A) Fluorescence intensity (□), initial phosphorescence intensity (●), and total phosphorescence intensity (○) are normalized and plotted as a function of $[I^-]$. (B) Derivation of the triplet yield from eq 4 as described in the text.

The quantum yield of triplet formation of α-crystallin in iodide-free solvent, ϕ_t^0, can be estimated from the data presented in Figure 6A. Following the analysis of Medinger and Wilkinson (1965) as summarized in Parker (1968):

$$\phi_f^0/\phi_f = [(D_T/D_T^0)(\phi_f^0/\phi_f) - 1](1 + k_{Q'}/k_Q)\phi_t^0 + 1 \quad (4)$$

where ϕ_f^0/ϕ_f is the ratio between the fluorescence quantum yield in iodide-free and iodide solutions, D_T/D_T^0 is the ratio of triplet formations, and $k_{Q'}$ and k_Q are the rate constants for $S_0 \leftarrow S_1$ and $T_1 \leftarrow S_1$ transitions upon quencher–fluorophore interaction. A plot of ϕ_f^0/ϕ_f vs $(D_T/D_T^0)(\phi_f^0/\phi_f) - 1$ is presented in Figure 6B. The slope [corresponding to $(1 + k_{Q'}/k_Q)\phi_t^0$] of the best linear fit to the data points was 0.05; hence, an upper bound of 5% is established for the triplet yield of α-crystallin.

Denaturation Studies. The fluorescence maximum and phosphorescence lifetime of α-crystallin were measured as a function of Gdn-HCl and urea concentration, and the results are presented in Figures 7 and 8. The fluorescence maximum shifts to longer wavelengths upon denaturation (Burstein et al., 1973), and the transition between the native and denatured states occurs between 1 and 2 M Gdn-HCl, and between 4 and 6 M urea.

A reduction in the lifetime of both the long- and short-lived components of the phosphorescence emission parallels the red shift of the fluorescence emission reflecting increased tryptophan mobility (Strambini & Gonnelli, 1985). In Gdn-HCl, the short-lived component decreases to a value of 300 μs at 2 M and then gradually decreases to ~100 μs in 6 M Gdn-HCl. The long-lived component decreases steadily to ~3 ms and retains this lifetime out to 6 M Gdn-HCl. Urea was a less effective denaturant. The long-lived component was abruptly reduced between 4.5 and 5 M urea, reaching a lifetime

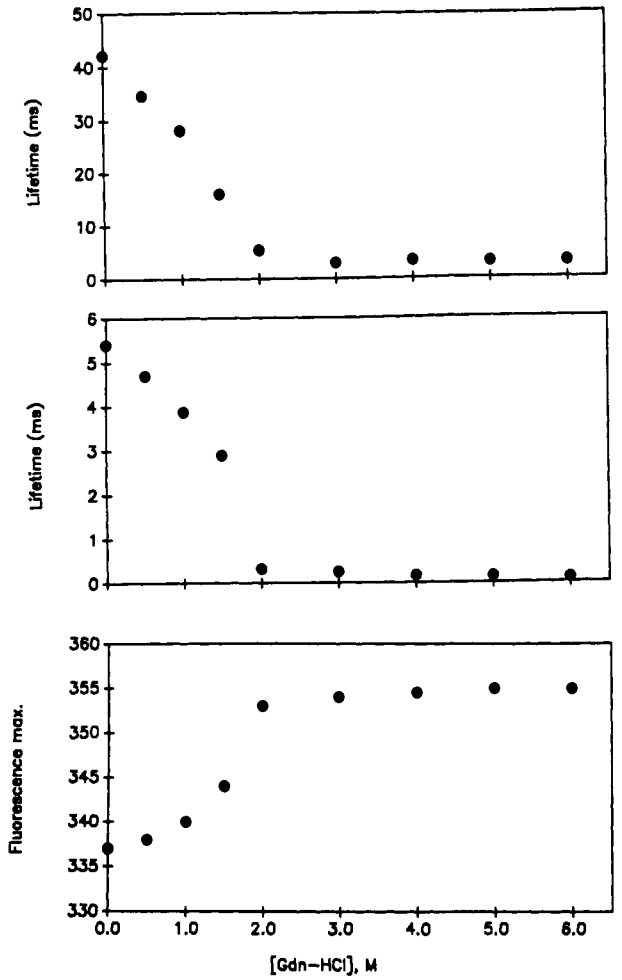

FIGURE 7: Denaturation behavior of α-crystallin in buffer/Gdn-HCl solutions. The long-lived (upper panel) and short-lived (middle panel) components of the phosphorescence emission and the spectral position of the fluorescence maximum (lower panel) are plotted versus denaturant concentration.

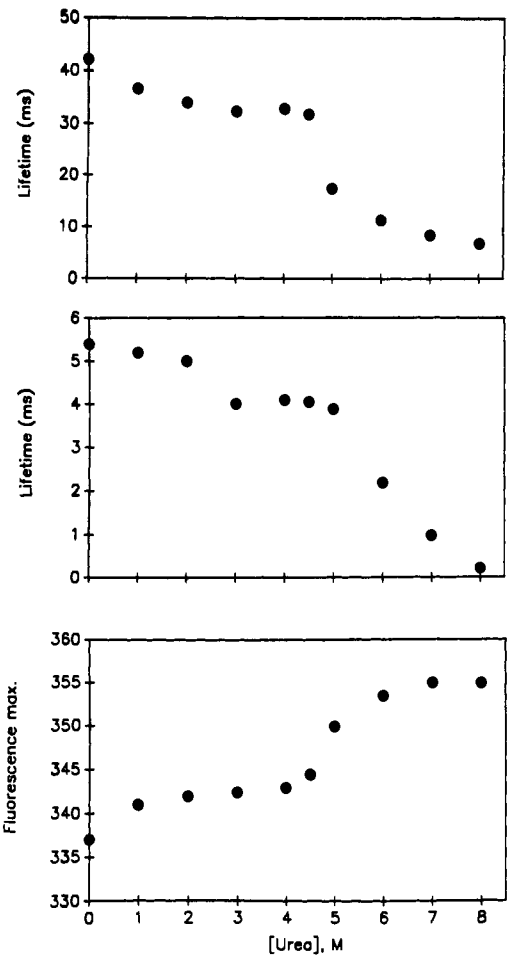

FIGURE 8: Denaturation behavior of α-crystallin in buffer/urea solutions. Data are presented as in Figure 7.

of 7 ms in 8 M urea, while the short-lived component exhibited a transition at 5–6 M urea, decreasing to ~200 μs in 8 M urea.

Discussion

Spectra. The spectral position of the fluorescence maximum varies considerably among tryptophan-containing proteins. Azurin with a fluorescence maximum at 308 nm has the bluest fluorescence emission, while free tryptophan and small polypeptides are known to fluoresce maximally at >350 nm (Longworth, 1971). The fluorescence emission of buried tryptophan residues is blue-shifted with respect to the emission of exposed tryptophans (Burstein et al., 1973), and this effect has been invoked to establish the relative exposures of Trp residues among lens crystallins (Borkman & Lerman, 1978; Liang & Chakrabarti, 1982; Liang et al., 1985). The fluorescence spectrum of bovine α-crystallin is consistent with tryptophan residues in a moderately hydrophobic environment.

Phosphorescence spectra are less sensitive to tryptophan microenvironment due to weak interactions between the solvent and the triplet state (Konev, 1967). At 77 K, most proteins phosphoresce with 0–0 peaks at 405–415 nm and secondary maxima at 435–441 nm (Longworth, 1971). Among lens crystallin proteins, only single, sharp 0–0 bands have been reported for α-crystallin (this work) and for γ-II, γ-III, and γ-IV crystallins (Berger et al., 1989); however, specific examples of spectral discrimination between tryptophan classes within a protein have been reported (Purkey & Galley, 1970). The phosphorescence spectra of proteins containing buried tryptophans are red-shifted with respect to the spectra of proteins containing partially exposed Trp residues (Longworth, 1971); hence, both the low-temperature and room temperature spectra are consistent with tryptophans in moderately hydrophobic microenvironments. Furthermore, the absence of appreciable splitting in the 0–0 band suggests that all Trp's reside in hydrophobic microenvironments, although variations in the degree of burial cannot be determined from phosphorescence spectral measurements.

Phosphorescence Lifetimes. The room temperature phosphorescence lifetime is determined by the frequency of radiationless transitions. Segmental flexibility and internal dynamics of tryptophan residues favor nonradiative deexcitation, and it has been proposed that tryptophan rigidity determines the phosphorescence lifetime at moderate temperatures (Strambini & Gonnelli, 1985). Internal dynamics vary greatly within a protein, and evidence suggests that buried tryptophans are more rigidly fixed than exposed Trp's (Karplus, 1986). Since intrasubunit interactions are the greatest determinant of tryptophan flexibility, it is likely that the three-dimensional arrangement of subunits within α-crystallin does not significantly influence the phosphorescence lifetime. Accumulating evidence suggests that the A and B subunits are structurally equivalent and occupy equivalent sites in all α-crystallin aggregates (Thomson & Augusteyn, 1988, 1989); hence, emission heterogeneity probably does not reflect the existence of multiple conformers. Furthermore, specific interactions between the aromatic amino acids of αA and αB subunits appear unlikely (Thomson & Augusteyn, 1989). In accordance with these observations, three unique classes of tryptophan residues

can be considered: Trp-A9, Trp-B9, and Trp-B60.

Two subpopulations of tryptophan residues were identified by unique phosphorescence lifetimes. Although we cannot rigorously exclude the unlikely possibility that only a fraction of the subunits contribute to the phosphorescence emission, the linearity of the Stern–Volmer quenching curves for both short- and long-lived phosphorescence components in all three quenchers supports the notion that each component corresponds to exactly one class of tryptophan residues. Several scenarios might account for the lack of a third contribution to the phosphorescence intensity decay. First, the half-width of the flashlamp excitation is 5–10 μs with a tail extending out to $\sim$100 μs; hence, our instrument would not detect a weak third component with $\tau_p < 100$ μs. Second, intramolecular quenching mechanisms might significantly reduce the intensity of one class of Trp residues. Finally, since the A and B subunits are 57% homologous (van der Ouderaa, 1974) and structurally equivalent (Thomson & Augusteyn, 1989), it is likely that the tryptophans at equivalent positions, i.e., Trp-A9 and -B9, are equally flexible and accessible, and phosphoresce with equal (or nearly equal) lifetimes. This explanation is most palatable; however, the assessment of these proposals and further interpretation await detailed structural information.

Temperature Dependence of the Phosphorescence Emission. The diminution of phosphorescence lifetime with increasing temperature is due to the increased efficiency of nonradiative transitions (Lin & Bersohn, 1968). At cryogenic temperatures, only the lowest vibrational states of the electronic excited state are populated; hence, relaxation processes originating solely from these states can contribute to radiationless deactivation. At higher temperatures, normal modes of the excited electronic state are populated providing additional pathways for radiationless decay (Lin & Bersohn, 1968). The temperature dependence of the rate constant for nonradiative decay (k_{nr}) can be expressed as

$$k_{nr} = k_{nr}^0 + \sum A_i \exp(-E_i/kT) \quad (5)$$

where k_{nr}^0 is the rate constant at $T = 0$ and A_i and E_i describe the temperature dependence of the deactivation for the ith relaxation process (Lin, 1972). At sufficiently low temperatures, the temperature dependence can be approximated by an Arrhenius equation of the form

$$k_{nr} = 1/\tau_p = 1/\tau_0 + (A/\tau_0) \exp(-E_a/kT) \quad (6)$$

and a linear Arrhenius plot would suggest that one deactivation process is dominant over the temperature range of interest.

Kai and Imakubo (1979) studied the temperature dependence of globular protein phosphorescence between 77 and 293 K. At 77 K, all proteins phosphoresced with $\tau_p = 5$–7 s. At higher temperatures, radiationless processes reduced the observed lifetime, with the onset of temperature-dependent deactivation occurring at $\sim$200 K. Arrhenius plots over the temperature-dependent range were linear and yielded activation energies of 8.0 $\pm$ 0.4 kcal/mol for all proteins considered, and A values from 7.3×10^5 s^{-1} for alkaline phosphatase to 2.5×10^9 s^{-1} for trypsin. It was argued that E_a is approximately constant for all proteins and that A characterizes the tryptophan microenvironment, low and high values of A corresponding to rigid and flexible tryptophans, respectively.

Below the transition temperatures T_c, our values for A and E_a are somewhat lower than typical values reported by Kai and Imakubo (1979), however, their protein samples were probably not sufficiently deoxygenated. Nitrogen bubbling did not fully deoxygenate the sample as evidenced by low room temperature phosphorescence lifetimes; the phosphorescence lifetimes reported for ribonuclease T1 (4 ms), aldolase (18 ms), and alkaline phosphatase (500 ms) are far lower than the currently accepted values of 14, 45, and 1500 ms, respectively (Vanderkooi et al., 1987). With this in mind, recalculation of the data presented in Kai and Imakubo would yield smaller values of E_a and A, consistent with our results for the long- and short-lived components of α-crystallin.

Above the transition temperature, additional deactivation pathways contribute to the overall relaxation. The discontinuities at 26 °C for the short-lived component and at 29 °C for the long-lived component most probably reflect abrupt transitions in segmental flexibility. Transient dichroism measurements of eosin-labeled proteins have identified abrupt segmental flexibility transitions in other systems (Hoffman et al., 1979; Junankar & Cherry, 1986); however, our measurements probe the flexibility of native unlabeled protein and reflect the dynamics of intrinsic residues.

Phosphorescence Quenching. The efficiency of fluorescence quenching by added small molecules such as acrylamide has been used to assess the exposure of tryptophan residues (Eftink & Ghiron, 1975, 1981). In addition, quenching studies of room temperature tryptophan phosphorescence have also yielded protein structural information, and the wide range of lifetimes and quenching constants allows for the discrimination of distinct contributions to the phosphorescence emission (Calhoun et al., 1988; Strambini, 1987). The mechanisms of fluorescence and phosphorescence quenching are not known with certainty; however, electron exchange, electron transfer, spin–orbit coupling, and Förster resonance energy transfer have been proposed to account for experimental evidence (Eftink & Ghiron, 1981; Calhoun et al., 1988). In principle, quenchers can interact with tryptophan residues through quencher penetration, partial tryptophan exposure, transient protein unfolding, or long-range mechanisms. Lakowicz and Weber (1973) suggested that O_2 can diffuse within a protein, and this penetration model has been extended to other quenchers and invoked to correlate the reduced quenching with tryptophan burial. Despite our limited understanding of quenching phenomena, it is true that buried tryptophans are less effectively quenched than exposed tryptophans.

The efficiency of luminescence quenching is determined by the nature of the quencher and the accessibility of the tryptophan indole ring. Acrylamide, nitrite, and iodide were chosen as quenchers in order to investigate the accessibility of α-crystallin tryptophans to dissimilar quenchers. Acrylamide (CH_2=$CHCONH_2$) is a small neutral molecule which has been shown to quench tryptophan fluorescence from both exposed and moderately buried residues. Nitrite (NO_2^-) is a small ionic quencher which also quenches tryptophan fluorescence with high efficiency. The iodide ion (I^-) is highly hydrated and quenches both fluorescence and phosphorescence with reduced efficiency, possibly due to size effects, charge effects, or differences in quenching mechanism.

Since rigidity and tryptophan burial are closely related, a strong correlation exists between long phosphorescence lifetimes and low bimolecular quenching constants (Calhoun et al., 1988). As seen in Table I, all three species quench the short-lived phosphorescence component more effectively than the long-lived phosphorescence component. Previous studies with γ-crystallins also exhibited this trend, and comparison between acrylamide phosphorescence quenching constants for α- and γ-II crystallins reveals differences in tryptophan accessibility. For γ-II crystallin, the quenching constants for the long- and short-lived components of the phosphorescence were 3.5×10 and 2.1×10^3 M^{-1} s^{-1} (Berger et al., 1989), respectively, confirming that the tryptophans in γ-II are more

buried than those in α-crystallin.

Among the three quenchers, acrylamide was most effective whereas iodide quenched the phosphorescence with an extremely small k_q. This result is consistent with fluorescence quenching measurements of α-crystallin where quenching constants of $\sim 1 \times 10^9$ and $(2-4) \times 10^8$ M^{-1} s^{-1} are reported for acrylamide and iodide quenching, respectively (Phillips et al., 1986; Augusteyn et al., 1988). In comparing nitrite with acrylamide, nitrite quenched with a lower k_q for both the long- and short-lived components of the phosphorescence emission, suggesting that negatively charged groups hinder the access of nitrite to the phosphorescing tryptophans (Lakowicz, 1983). Phillips et al. (1986) and Augusteyn et al. (1988) observed a downward curvature in the Stern–Volmer plots for fluorescence quenching by both acrylamide and iodide indicative of selective quenching and suggesting the existence of at least two subpopulations of tryptophan residues with markedly different accessibilities. It was speculated that two classes of tryptophan contribute to the fluorescence emission: one class corresponding to Trp-A9 and Trp-B9 and the other to Trp-B60 (Augusteyn et al., 1988). Our phosphorescence measurements support this notion and unambiguously identify two distinct classes of Trp residues, with the more buried class having the longer emission lifetime.

Iodide Heavy-Atom Effect. Heavy atoms perturb spin–orbit coupling and promote intersystem crossing (Turro, 1978; Lessard & Durocher, 1979). Iodide-containing solvents have been shown to promote triplet formation at low temperatures (Parker, 1968; Turro, 1978); however, heavy-atom enhancement of room temperature protein phosphorescence has not been previously demonstrated. The initial phosphorescence intensity relates directly to triplet formation, while the total phosphorescence intensity reflects the interplay between enhanced $T_1 \leftarrow S_1$ intersystem crossing, and phosphorescence quenching by iodide.

We derive an upper bound of 5% for the triplet yield of α-crystallin at 293 K. Although the mechanism of fluorescence quenching by iodide is not known with certainty, it is presumed that heavy-atom-enhanced intersystem crossing contributes to the depletion of the excited singlet state (Monsigny et al., 1978). If the mechanism of fluorescence quenching is exclusively via $T_1 \leftarrow S_1$ transitions, then $k_{Q'} \ll k_Q$, and the triplet yield is 5%. Alternately, if iodide also acts to promote $S_0 \leftarrow S_1$ transitions, then the true triplet yield will be less than the estimated value of 5%. For example, if $k_Q = k_{Q'}$, then $\Phi_t^0 = 2.5\%$. Hence, as noted, 5% is an upper bound for the efficiency of triplet formation.

Longworth (1971) reports phosphorescence yields of 3–15% for tryptophan-containing proteins at 77 K. The phosphorescence yield at room temperature, Φ_p, can be estimated with the assumption of a temperature-independent rate of intersystem crossing. Following the analysis of Parker (1968):

$$\tau_{RT}/\tau_0 = \Phi_p/\Phi_0 \quad (7)$$

where τ_0 and Φ_0 are the phosphorescence lifetime and quantum yield at 77 K, respectively. Representative values of $\tau_0 = 5$ s and $\Phi_0 = 0.1$ are derived from the literature, and τ_{RT} is the weighted average of the room temperature phosphorescence lifetimes ($\tau_{RT} = 16$ ms), yielding $\Phi_p \sim 3.2 \times 10^{-4}$. As expected, there is considerable deactivation of the triplet state at room temperature, resulting in a low phosphorescence quantum yield.

Denaturation Studies. The data of Figures 7 and 8 demonstrate the differential effectiveness of urea and Gdn-HCl as denaturation agents for α-crystallin. The principal transition between the native and denatured states occurs between 4 and 6 M urea, and between 1 and 2 M Gdn-HCl. As expected, the denaturation of α-crystallin in 8 M urea is less complete than in 6 M Gdn-HCl; whereas phosphorescence lifetimes of 100 μs and 3 ms were observed in 6 M Gdn-HCl, lifetimes of 200 μs and 7 ms were measured in 8 M urea.

In Figure 7, a gradual denaturation between 0 and 2 M Gdn-HCl concomitant with a reduction in phosphorescence lifetime is observed. At low concentrations of Gdn-HCl, the phosphorescence lifetime decreases, reflecting loosened intramolecular associations and enhanced segmental flexibility (Strambini & Gonnelli, 1986), and this effect is observed for both the long- and short-lived components of the phosphorescence emission. The increase in segmental flexibility between 0 and 2 M Gdn-HCl is in agreement with fluorescence polarization studies of fluorescein-labeled α-crystallin, which exhibited a sharp decrease in the rotational relaxation time between 0 and 2 M Gdn-HCl indicative of increased segmental flexibility (Liang & Pelletier, 1988). At high concentrations of Gdn-HCl, conformational changes are induced. The lifetime of the short-lived component decreases further, while the long-lived component maintains a lifetime of 3 ms, suggesting that some structure is preserved even at 6 M Gdn-HCl. In addition, although the tryptophans in the denatured proteins most likely exist in a broad distribution of microenvironments, both fast and slow decay components were detected, reflecting flexibility heterogeneity in 6 M Gdn-HCl. While fluorescence measurements indicate that the Trp's are solvent-exposed, phosphorescence measurements clearly identify rigidity differences among the tryptophans.

In urea, a gradual loosening between 0 and 4 M is followed by a more abrupt transition between 4 and 6 M. The long-lived component exhibits a transition between 4.5 and 5 M, while the short component transition occurs between 5 and 6 M urea. This result suggests that the structural features preserving the highly buried tryptophans are perturbed prior to the disruption of the more exposed tryptophan subpopulation. At 8 M urea, the lifetime of the long-lived component is 7 ms which again suggests that some rigidity is preserved even at very high denaturant concentrations.

Conclusions. Our studies demonstrate the exquisite sensitivity of room temperature phosphorescence measurements to the structure and conformation of lens α-crystallin. Fluorescence quenching measurements suggest that two classes of tryptophan residues contribute to the emission (Phillips et al., 1986; Augusteyn et al., 1988), and our results unambiguously confirm this notion. The wide range of phosphorescence lifetimes and quenching constants allows for the discrimination of distinct tryptophan subpopulations, and our studies demonstrate differences in flexibility and accessibility. In addition, temperature-dependent and denaturant-dependent dynamic changes could be detected by simultaneously monitoring each of the two observable subpopulations, demonstrating the applicability of room temperature phosphorescence spectroscopy for monitoring conformational changes of lens crystallin proteins.

References

Andley, U. P., & Chapman, S. F. (1986) *Photochem. Photobiol. 44*, 67–74.

Augusteyn, R. C., Putilina, T., & Seifert, R. (1988) *Curr. Eye Res. 7*, 237–245.

Berger, J. W., Vanderkooi, J. M., Tallmadge, D. H., & Borkman, R. F. (1989) *Exp. Eye Res.* (in press).

Bloemendal, H. (1981) in *Molecular and Cellular Biology of the Eye Lens* (Bloemendal, H., Ed.) pp 1–47, Wiley, New York.

Borkman, R. F., & Lerman, S. (1978) *Exp. Eye Res. 26*, 705–713.
Burstein, E. A., Vedenkina, N. S., & Ivkova, M. N. (1973) *Photochem. Photobiol. 18*, 263–279.
Calhoun, D. B., Englander, S. W., Wright, W. W., & Vanderkooi, J. M. (1988) *Biochemistry 27*, 8466–8474.
Chiesa, R., Gawinowicz-Kolks, M. A., Kleiman, N. J., & Spector, A. (1988) *Exp. Eye Res. 46*, 199–208.
Eftink, M. R., & Ghiron, C. A. (1975) *Proc. Natl. Acad. Sci. U.S.A. 72*, 3290–3294.
Eftink, M. R., & Ghiron, C. A. (1981) *Anal. Biochem. 114*, 199–227.
Englander, S. W., Calhoun, D. B., & Englander, J. J. (1987) *Anal. Biochem. 161*, 300–306.
Green, T. J., Wilson, D. F., Vanderkooi, J. M., & DeFeo, S. P. (1988) *Anal. Biochem. 174*, 73–79.
Harding, J. J. (1972) *Biochem. J. 129*, 97–100.
Harding, J. J. (1981) in *Molecular and Cellular Biology of the Eye Lens* (Bloemendal, H., Ed.) pp 327–365, Wiley, New York.
Hoffman, W., Sarzala, M. G., & Chapman, D. (1979) *Proc. Natl. Acad. Sci. U.S.A. 76*, 3860–3864.
Junankar, P. P., & Cherry, R. J. (1986) *Biochim. Biophys. Acta 854*, 198–206.
Kai, Y., & Imakubo, K. (1979) *Photochem. Photobiol. 29*, 261–265.
Karplus, M. (1986) *Methods Enzymol. 131*, 283–307.
Kishner, S., Trepman, W., & Galley, W. C. (1983) *Can. J. Biochem. 57*, 1299–1304.
Konev, S. (1967) *Fluorescence and Phosphorescence of Proteins and Nucleic Acids*, Plenum Press, New York.
Laemmli, U. K. (1970) *Nature (London) 227*, 680–685.
Lakowicz, J. R. (1983) *Principles of Fluorescence Spectroscopy*, Plenum Press, New York.
Lakowicz, J. R., & Weber, G. (1973) *Biochemistry 12*, 4171–4179.
Lerman, S., & Borkman, R. F. (1978) *Interdiscip. Top. Gerontol. 13*, 154–182.
Lessard, G., & Durocher, G. (1979) *Photochem. Photobiol. 29*, 399–402.
Liang, J. N. (1987) *Curr. Eye Res. 6*, 351–355.
Liang, J., & Chakrabarti, B. (1981) *Biochem. Biophys. Res. Commun. 102*, 180–189.
Liang, J., & Chakrabarti, B. (1982) *Biochemistry 21*, 1847–1852.
Liang, J. N., & Pelletier, M. R. (1988) *Exp. Eye Res. 46*, 745–752.
Liang, J. N., Andley, U. P., & Chylack, L. T. (1985) *Biochim. Biophys. Acta 832*, 197–203.
Liang, J. N., Hershorin, L. L., & Chylack, L. T. (1986) *Diabetologica 29*, 225–228.
Libondi, T., Magnante, P., Chylack, L. T., & Benedek, G. B. (1986) *Curr. Eye Res. 5*, 411–419.
Lin, S. H. (1972) *J. Chem. Phys. 56*, 2648–2653.
Lin, S. H., & Bersohn, R. (1968) *J. Chem. Phys. 48*, 2732–2736.
Longworth, J. W. (1971) in *Excited States of Proteins and Nucleic Acids* (Steiner, R. F., & Weinryb, I., Eds.) pp 319–484, Plenum Press, New York.
Mandal, K., Kono, M., Bose, S. K., Thomson, J., & Chakrabarti, B. (1988) *Photochem. Photobiol. 47*, 583–591.
McNamara, M. K., & Augusteyn, R. C. (1984) *Curr. Eye Res. 3*, 571–583.
Medinger, T., & Wilkinson, F. (1965) *Trans. Faraday Soc. 61*, 620–630.
Monsigny, M., Delmotte, F., & Helene, C. (1978) *Proc. Natl. Acad. Sci. U.S.A. 75*, 1324–1328.
Ozaki, Y., Mizuno, A., Itoh, K., Yoshiura, M., Iwamoto, T., & Iriyama, K. (1983) *Biochemistry 22*, 6254–6259.
Parker, C. A. (1968) *Photoluminescence of Solutions*, Elsevier Publishing Co., Amsterdam.
Phillips, S. R., Wilson, L. J., & Borkman, R. F. (1986) *Curr. Eye Res. 5*, 611–619.
Purkey, R. M., & Galley, W. C. (1970) *Biochemistry 9*, 3569–3575.
Saviotti, M. L., & Galley, W. C. (1974) *Proc. Natl. Acad. Sci. U.S.A. 71*, 4154–4158.
Siezen, R. J., Bindels, J. C., & Hoenders, H. J. (1980) *Eur. J. Biochem. 111*, 435–444.
Strambini, G. B. (1987) *Biophys. J. 52*, 23–28.
Strambini, G. B., & Gonnelli, M. (1985) *Chem. Phys. Lett. 115*, 196–200.
Strambini, G. B., & Gonnelli, M. (1986) *Biochemistry 25*, 2471–2476.
Strambini, G. B., Cioni, P., & Felicioli, R. A. (1987) *Biochemistry 26*, 4968–4975.
Tardieu, A., & Delaye, M. (1988) *Annu. Rev. Biophys. Biophys. Chem. 17*, 47–70.
Tardieu, A., Laporte, D., Licinio, P., Krop, B., & Delaye, M. (1986) *J. Mol. Biol. 192*, 711–724.
Thomson, J. A., & Augusteyn, R. C. (1988) *Curr. Eye Res. 7*, 563–569.
Thomson, J. A., & Augusteyn, R. C. (1989) *Biochim. Biophys. Acta 994*, 246–252.
Turro, N. J. (1978) *Modern Molecular Photochemistry*, Benjamin/Cummings, Menlo Park, CA.
Vanderkooi, J. M., Calhoun, D. B., & Englander, S. W. (1987) *Science 236*, 568–569.
van der Ouderaa, F. J., de Jong, W. W., & Bloemendal, H. (1973) *Eur. J. Biochem. 39*, 207–222.
van der Ouderra, F. J., de Jong, W. W., Hilderink, A., & Bloemendal, H. (1974) *Eur. J. Biochem. 49*, 157–168.
van Kleef, F. S. M., Willems-Thijssen, W., & Hoenders, H. J. (1976) *Eur. J. Biochem. 66*, 477–483.